SUPPLEMENTARY MATERIAL: SYSTEM DYNAMICS AND CHARACTERISTICS OF OPTIMAL CONTROL

Dynamics of Core Control System

The signaling network shown in FIG. 1 is simplified by keeping miR-451 in one module and merging all complex network between CAB39/LKB1/STRAD and AMPK into another module. The mathematical model takes into account signaling source and autocatalytic activities of miR-451 and the AMPK complex, mutual antagonism between miR-451 module and AMPK complex, and microRNA/protein degradation of those key molecules. FIG. 2A illustrates the conceptual model of the signaling pathways indicating mutual inhibition between miR-451 and AMPK complex [1, 2].

Based on biological observations in [2, 3], phenomenological equations for the rate change of those key molecules have the following dimensionless form [see 1, Appendix A]:

$$
\begin{aligned}
\frac{dM}{dt} &= G + \frac{k_1 k_2^2}{k_2^2 + \alpha A^2} - M, \\
\varepsilon \frac{dA}{dt} &= S + \frac{k_3 k_4^2}{k_4^2 + \beta M^2} - A,
\end{aligned}
\tag{1}
$$

where G represents glucose levels, S represents signaling strength to the module of AMPK complex, and $k_1, k_2, k_3, k_4, \alpha, \beta, \varepsilon$ are non-negative essential parameters. Note that the dimensionless parameter α controls the inhibition strength of miR-451 (M) by the AMPK complex (A), and the dimensionless parameter β controls the inhibition strength of the AMPK complex (A) by miR-451 (M). A small parameter ε is due to the different degradation rates of miR-451 and protein AMPK. The schematic dimensionless network is shown in FIG. 2B.

FIGs. 3A-3C show the different nullclines and vector fields of the given system (1) for low ($G = 0.01$), intermediate ($G = 0.45$), and high ($G = 1.0$) glucose levels, respectively. Different levels of glucose lead to different behaviors of steady states (SS). The low glucose level (G=0.01) induces only one SS on the upper-left corner of the $M - A$ domain. This down-regulated miR-451 level and increased AMPK activity activate the migratory status of the glioma cell. In contrast, the up-regulated miR-451 level and lowered AMPK activity, leading to a proliferative mode [2, 3] can be induced under high glucose levels ($G = 1.0$) (see FIG. 3C; unique SS in the lower-right corner of the $M - A$ domain). This led to a following characterization of the proliferative (Z_p) and migratory zones (Z_m) by taking the thresholds, th_M (= 2.0) of miR-451 levels and th_A (=2.0) of AMPK complex [1, 4] (see FIG. 3E):

$$
\begin{aligned}
Z_p &= \{(M, A) \in \mathbb{R}^2 : M > th_M, \ A < th_A\}, \\
Z_m &= \{(M, A) \in \mathbb{R}^2 : M < th_M, \ A > th_A\}.
\end{aligned}
\tag{2}
$$

For an intermediate glucose level ($G = 0.45$), the core control system generates a bistable behavior: two stable SS (two black filled circles; one in the proliferative zone and one in the migratory region) and one unstable SS in the middle (black hollow circle). See FIG. 3B. Based on these observations, one can get a bifurcation curve, specifically hysteresis (FIG. 3D), *i.e.,* the steady state values of the miR-451 level (M^s) with glucose level parameter G. When G is low, system (1) is in the lower branch and glioma cells are in a migratory phase, but for high G, it is in the upper branch and glioma cells proliferate. The hysteresis effect represents history-dependence as the glucose level is varied. Glioma cells are migrating if the glucose level is increasing along the lower branch and proliferating if the glucose level is decreasing along the upper branch. This bistability of miR-451/AMPK being regulated by the glucose level allows us to formulate the control problem. Specifically, we aim to confine miR-451 levels in its proliferative state, a stable upper branch in the hysteresis dynamics prohibiting cells to migrate and invade surrounding tissues while regulating the amount of glucose and/or drug intravenous infusions at the same time keeping the cost of administrations as minimum as possible.

Non-dimensionalization of the Extended Model

The four key players of the intracellular structure are glucose level (g), miR-451 level (m), AMPK complex activity (a), and concentration of drugs (c). Kinetic interpretation of arrows and hammerheads in the network represents induction and inhibition, respectively. Then, the phenomenological equations for the rate change of concentrations of glucose and those key molecules

(m, a, c) are as follows:

$$\frac{dg}{dt} = U - \mu_g g,$$

$$\frac{dm}{dt} = \lambda_g g + \frac{\Lambda_1 \Lambda_2^2}{\Lambda_2^2 + \Lambda_5 \eta(c) F(a)} - \mu_1 m,$$

$$\frac{da}{dt} = s + \frac{\Lambda_3 \Lambda_4^2}{\Lambda_4^2 + \Lambda_6 H(m)} - \mu_2 a,$$

$$\frac{dc}{dt} = s_c - \mu_c c,$$

(3)

where U is the glucose source from blood or infusion, s is the signaling pathways to AMPK complex, s_c is the signal source of drug (c), λ_g is the signaling strength from glucose to miR-451, Λ_1, Λ_3 are the autocatalytic enhancement parameters for miR-451 and AMPK complex, respectively, Λ_2, Λ_4 are the Hill-type inhibition saturation parameters from the counter part of miR-451 and AMPK complex, respectively, Λ_5 is the inhibition strength of miR-451 by the AMPK complex, Λ_6 is the inhibition strength of the AMPK complex by miR-451, μ_g is the decay/consumption rate of glucose, μ_1, μ_2 are microRNA/protein degradation rates of miR-451 and AMPK complex, respectively, and μ_c is the degradation/decay rate of drug. Here, we introduce inhibition strength function $\eta(c)$ in the denominator of the right hand side of dm/dt. AMPK-dependent inhibition of miR-451 is through the function $F(a)$ and miR-451-dependent inhibition of AMPK complex is through the function $H(m)$. A requirement on these functions are that $\frac{\partial F}{\partial a} > 0$ for all non-negative a and $\frac{\partial H}{\partial m} > 0$ for all non-negative m. Following the arguments and assumptions in [1, 4], we have

$$F(a) = a^2, \; H(m) = m^2.$$

(4)

System (3) can be non-dimensionalized using

$$T = \mu_1 t, \; M = \frac{m}{m^*}, \; A = \frac{a}{a^*}, \; G = \frac{g}{m^*}, D = \frac{c}{c^*}, \; g = \frac{U}{\mu_1 m^*}, \; \lambda_g = \frac{\Lambda_g}{\mu_1}, \; S = \frac{s}{\mu_2 a^*},$$

$$d = \frac{s_c}{\mu_1 c^*}, \; k_1 = \frac{\Lambda_1}{\mu_1 m^*}, \; k_2 = \Lambda_2, \; k_3 = \frac{\Lambda_3}{\mu_2 a^*}, \; k_4 = \Lambda_4, \; \alpha = \Lambda_5 (a^*)^2,$$

$$\beta = \Lambda_6 (m^*)^2, \; \varepsilon = \frac{\mu_1}{\mu_2}, \; \mu = \frac{\mu_g}{\mu_1}, \; \delta = \frac{\mu_c}{\mu_1}, \; \zeta(D) = \eta(c),$$

(5)

so that the network can be lumped into a smaller set of essential control parameters.

Characteristics of Optimal Control

As reported in [4], fluctuating glucose supply leads to dichotomy between cell proliferation and migration resulting to faster growth of tumor mass. Optimal control theory is used to explore strategies in maintaining high levels of up-regulated miR-451 concentrations keeping glioma cells in proliferative mode and thus preventing them from invading other parts of brain tissue. On the other hand, expenses on glucose and drug administrations are minimized in terms of frequency and dose of infusion. Let $u_1(t)$ and $u_2(t)$ denote the controls of the system representing dose rate of glucose and drug intravenous administrations, respectively. We have considered the following three different control strategies under different circumstances in order to achieve our goal.

Strategy I: glucose infusion control $u_1(t)$

$$\text{with} \quad \begin{cases} \dfrac{dG}{dt} = u_1(t) - \mu G, \\[2mm] \dfrac{dM}{dt} = G + \dfrac{k_1 k_2^2}{k_2^2 + \alpha A^2} - M, \\[2mm] \varepsilon \dfrac{dA}{dt} = S + \dfrac{k_3 k_4^2}{k_4^2 + \beta M^2} - A, \end{cases}$$

(6)

Strategy II: glucose infusion control $u_1(t)$ with drug intervention

$$\text{with} \quad \begin{cases} \dfrac{dG}{dt} &= u_1(t) - \mu G, \\[2mm] \dfrac{dM}{dt} &= G + \dfrac{k_1 k_2^2}{k_2^2 + \alpha e^{-D} A^2} - M, \\[2mm] \varepsilon \dfrac{dA}{dt} &= S + \dfrac{k_3 k_4^2}{k_4^2 + \beta M^2} - A, \\[2mm] \dfrac{dD}{dt} &= d - \delta D, \end{cases} \tag{7}$$

Strategy III: glucose infusion control $u_1(t)$ and drug infusion control $u_2(t)$

$$\text{with} \quad \begin{cases} \dfrac{dG}{dt} &= u_1(t) - \mu G, \\[2mm] \dfrac{dM}{dt} &= G + \dfrac{k_1 k_2^2}{k_2^2 + \alpha e^{-D} A^2} - M, \\[2mm] \varepsilon \dfrac{dA}{dt} &= S + \dfrac{k_3 k_4^2}{k_4^2 + \beta M^2} - A, \\[2mm] \dfrac{dD}{dt} &= u_2(t) - \delta D. \end{cases} \tag{8}$$

The objective functional J is defined by

$$J(u_1(t), u_2(t)) = \int_{t_0}^{t_1} \left[M(t) - \left(\frac{B_1}{2} u_1(t)^2 + \frac{B_2}{2} u_2(t)^2 \right) \right] dt, \tag{9}$$

where $M(t)$ denotes the level of miR-451 concentration, and $u_1(t), u_2(t)$ are the glucose and drug infusion controls, respectively. Parameters B_1 and B_2 are weight factors measuring the relative cost based on maximizing $M(t)$ and administering glucose and drug intravenous infusions over $[t_0, t_1]$, respectively. The control costs are modeled via linear combination of quadratic terms, $u_i^2(t)$, $i = 1, 2$. The goal is to find optimal control(s) $u_1^*(t)$ and $u_2^*(t)$ such that

$$J(u_1^*(t), u_2^*(t)) = \max_{\Omega} J(u_1(t), u_2(t)), \tag{10}$$

where

$$\Omega = \left\{ (u_1(t), u_2(t)) \in \mathscr{L}^2(t_0, t_1)^2 \,|\, 0 \leq u_1(t), u_2(t) \leq u_{\max}, \ t \in [t_0, t_1] \right\}. \tag{11}$$

The bounds for controls stand for the limit on dose rates of glucose and drug administrations.

Assuming that miR-451 and AMPK responses are regulated by glucose levels, the first strategy deals with finding an optimal control regimen for glucose intravenous infusion. In the second strategy, we are concerned with optimizing glucose intravenous infusion only taking into account inexpensive and readily available drug. This drug is assumed to be administered concomitantly with glucose as a secondary intravenous infusion. The last strategy applies to minimize the cost incurred in glucose and drug administrations considering an invaluable efficacy but expensive and scarce drug. The scheme tries to find a control regimen for both glucose and drug intravenous infusions.

We note that the existence of optimal controls is guaranteed by standard results in control theory [5]. In this maximization problem, the necessary convexity of the integrand of objective functional holds. Therefore, we can proceed with applying Pontryagin's Maximum Principle [6]. The following theorems are obtained corresponding to three control strategies mentioned above.

Theorem 1. *There exists an optimal control $u_1^*(t)$ and corresponding solutions $G^*(t), M^*(t), A^*(t)$ that maximize the objective functional*

$$J(u_1(t)) = \int_{t_0}^{t_1} \left(M(t) - \frac{B_1}{2} u_1(t)^2 \right) dt, \tag{12}$$

over $\{u_1(t) \in \mathcal{L}^2(t_0, t_1) | 0 \le u_1(t) \le u_{\max}\}$. *Given this optimal solution, there exist adjoint equations satisfying*

$$\frac{d\lambda_1}{dt} = \mu\lambda_1 - \lambda_2 ,$$

$$\frac{d\lambda_2}{dt} = -1 + \lambda_2 + \frac{1}{\varepsilon} \frac{2k_3 k_4^2 \beta M}{\left(k_4^2 + \beta M^2\right)^2} \lambda_3 ,$$

$$\frac{d\lambda_3}{dt} = \frac{2k_1 k_2^2 \alpha A}{\left(k_2^2 + \alpha A^2\right)^2} \lambda_2 + \frac{1}{\varepsilon}\lambda_3 ,$$

(13)

with transversality conditions

$$\lambda_i(t_1) = 0, \qquad i = 1, 2, 3. \tag{14}$$

Furthermore,

$$u_1^*(t) = \min\left(b, \max\left(a, \frac{\lambda_1}{B}\right)\right) , \tag{15}$$

where $a = 0$, and $b = u_{\max}$.

Theorem 2. *There exists an optimal control $u^*(t)$ and corresponding solutions $G^*(t)$, $M^*(t)$, $A^*(t)$, $D^*(t)$ that maximize the objetive functional (12) over $u_1(t) \in \mathcal{L}^2(t_0, t_1)$ such that $0 \le u_1(t) \le u_{\max}$. Given this optimal solution, there exist adjoint equations satisfying*

$$\frac{d\lambda_1}{dt} = \mu\lambda_1 - \lambda_2 ,$$

$$\frac{d\lambda_2}{dt} = -1 + \lambda_2 + \frac{1}{\varepsilon} \frac{2k_3 k_4^2 \beta M}{\left(k_4^2 + \beta M^2\right)^2} \lambda_3 ,$$

$$\frac{d\lambda_3}{dt} = \frac{2k_1 k_2^2 \alpha e^{-D} A}{\left(k_2^2 + \alpha e^{-D} A^2\right)^2} \lambda_2 + \frac{1}{\varepsilon}\lambda_3 ,$$

$$\frac{d\lambda_4}{dt} = -\frac{k_1 k_2^2 \alpha e^{-D} A^2}{\left(k_2^2 + \alpha e^{-D} A^2\right)^2} \lambda_2 + \mu_2 \lambda_4 ,$$

(16)

with transversality conditions

$$\lambda_i(t_1) = 0, \qquad i = 1, 2, 3, 4. \tag{17}$$

Furthermore,

$$u_1^*(t) = \min\left(b, \max\left(a, \frac{\lambda_1}{B}\right)\right) , \tag{18}$$

where $a = 0$, and $b = u_{\max}$.

Theorem 3. *There exist optimal controls $u_1^*(t), u_2^*(t)$ and corresponding solutions $G^*(t), M^*(t), A^*(t), D^*(t)$ that maximize the objective functional (9) over $(u_1(t), u_2(t))$ in $\mathcal{L}^2(t_0, t_1)^2$ with $0 \le u_1(t), u_2(t) \le u_{\max}$. Given these optimal solutions, there exist adjoint equations satisfying*

$$\frac{d\lambda_1}{dt} = \mu\lambda_1 - \lambda_2 ,$$

$$\frac{d\lambda_2}{dt} = -1 + \lambda_2 + \frac{1}{\varepsilon} \frac{2k_3 k_4^2 \beta M}{\left(k_4^2 + \beta M^2\right)^2} \lambda_3 ,$$

$$\frac{d\lambda_3}{dt} = \frac{2k_1 k_2^2 \alpha e^{-D} A}{\left(k_2^2 + \alpha e^{-D} A^2\right)^2} \lambda_2 + \frac{1}{\varepsilon}\lambda_3 ,$$

$$\frac{d\lambda_4}{dt} = -\frac{k_1 k_2^2 \alpha e^{-D} A^2}{\left(k_2^2 + \alpha e^{-D} A^2\right)^2} \lambda_2 + \mu_2 \lambda_4 ,$$

(19)

with transversality conditions

$$\lambda_i(t_1) = 0, \qquad i = 1,2,3,4. \tag{20}$$

Furthermore,

$$u_1^*(t) = \min\left(b, \max\left(a, \frac{\lambda_1}{B_1}\right)\right),$$
$$u_2^*(t) = \min\left(b, \max\left(a, \frac{\lambda_4}{B_2}\right)\right), \tag{21}$$

where $a = 0$, and $b = u_{\max}$.

Proof. The convexity of the integrand of objective functional guarantees the existence of optimal controls u_1^* and u_2^*. Applying Pontryagin's Maximum principle [6] converts our maximization problem (10) into maximizing the Hamiltonian given by

$$H = M - \frac{B_1}{2}u_1^2 - \frac{B_2}{2}u_2^2 + \lambda_1(u_1 - \mu G) + \lambda_2\left(G + \frac{k_1 k_2^2}{k_2^2 + \alpha e^{-D}A^2} - M\right)$$
$$+ \lambda_3\left(\frac{1}{\varepsilon}\left(S + \frac{k_3 k_4^2}{k_4^2 + \beta M^2} - A\right)\right) + \lambda_4(u_2 - \delta D).$$

The following adjoint equations and transversality conditions are obtained:

$$\frac{d\lambda_1}{dt} = -\frac{\partial H}{\partial G}, \qquad \lambda_1(t_1) = 0,$$
$$\frac{d\lambda_2}{dt} = -\frac{\partial H}{\partial M}, \qquad \lambda_2(t_1) = 0,$$
$$\frac{d\lambda_3}{dt} = -\frac{\partial H}{\partial A}, \qquad \lambda_3(t_1) = 0,$$
$$\frac{d\lambda_4}{dt} = -\frac{\partial H}{\partial D}, \qquad \lambda_4(t_1) = 0.$$

After differentiating H with respect to the control u_1 and u_2 and considering the bounds give the following characterization of the controls, respectively

$$u_1^*(t) = \min\left(b, \max\left(a, \frac{\lambda_1}{B_1}\right)\right),$$
$$u_2^*(t) = \min\left(b, \max\left(a, \frac{\lambda_4}{B_2}\right)\right). \tag{22}$$

□

The proofs of the first two theorems follow the same arguments as presented in the proof of third theorem with modifications on objective functional, adjoint and optimality equations .

---

[1] Kim, Y. & Roh, S. 2013 A hybrid model for cell proliferation and migration in glioblastoma. *Discrete Contin. Dyn. Syst. Ser. B* **18**, 969–1015. (doi:10.3934/dcdsb.2013.18.969)

[2] Godlewski, J., Nowicki, M. O., Bronisz, A., Nuovo, G., Palatini, J., De Lay, M., Van Brocklyn, J., Ostrowski, M. C., Chiocca, E. A., & Lawler, S.E. 2010 MicroRNA-451 regulates LKB1/AMPK signaling and allows adaptation to metabolic stress in glioma cells. *Mol. Cell* **37**, 620–632. (doi: 10.1016/j.molcel.2010.02.018)

[3] Godlewski, J., Bronisz, A., Nowicki, M. O., Chiocca, E. A. & Lawler, S. 2010 microRNA-451: A conditional switch controlling glioma cell proliferation and migration. *Cell Cycle* **9**, 2742–2748.

[4] Kim, Y., Roh, S., Lawler, S. & Friedman, A. 2011 miR451 and AMPK mutual antagonism in glioma cell migration and proliferation: a mathematical model. *PLoS One* **6**, e28293. (doi: 10.1371/journal.pone.0028293)

[5] Fleming, W. H. & Rishel, R. W. 1975 Deterministic and Stochastic Optimal Control. *Springer Verlag, New York.*

[6] Pontryagin, L. S., Boltyanskii, V. G., Gamkrelidze, R. V. & Mishchenko, E. F. 1962 The mathematical theory of optimal processes. *New Jersey: Wiley.*
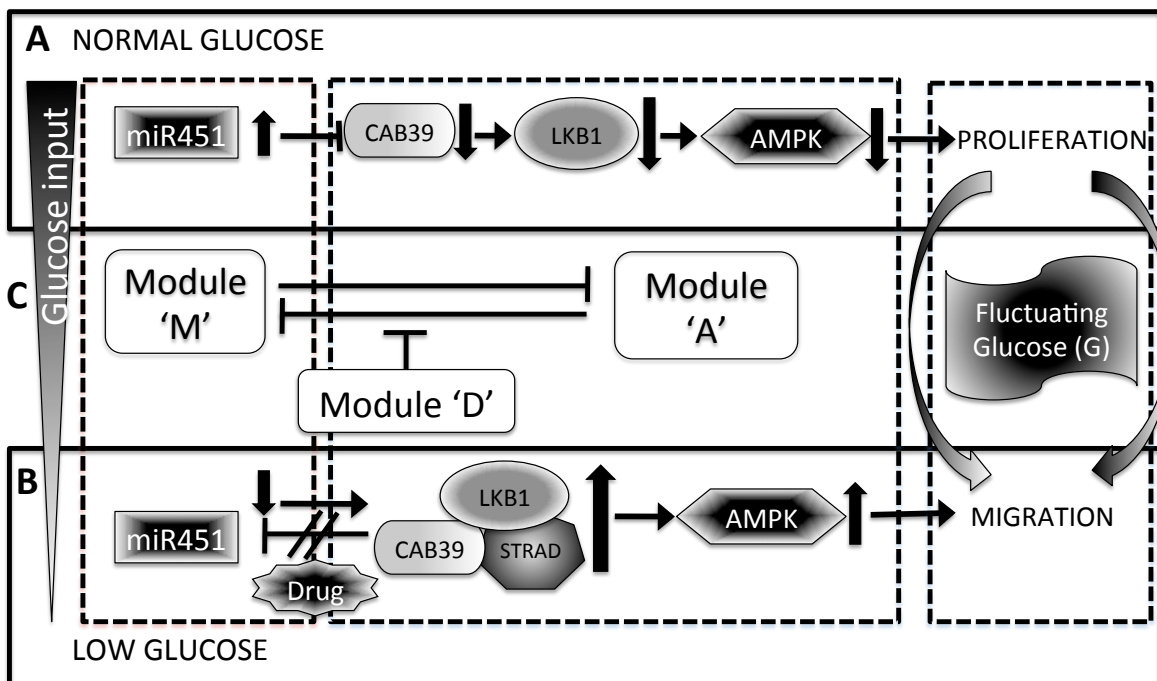
FIG. 1. Mutual antagonism between miR-451 and the AMPK complex in the regulation of cell proliferation and migration in response to high and low glucose levels [4]. miR-451 levels determine cell proliferation and migration in response to fluctuating glucose via the AMPK signaling network [2]. (A) Normal (high) glucose levels up-regulate miR-451 and down-regulate AMPK activity (CAB39/LKB1/AMPK), leading to increased proliferation and decreased cell migration. (B) Low glucose levels decrease the miR-451 level and increase the levels of the AMPK complex, leading to reduced cell proliferation and enhanced cell motility (C) Schematic components of miR-451 and CAB39/LKB1/AMPK complex are represented by modules 'M' and 'A', respectively, in our theoretical framework. Schematic component of possible drugs blocking the inhibitory pathway of the miR-451 module by the AMPK complex is represented by a module 'D' .
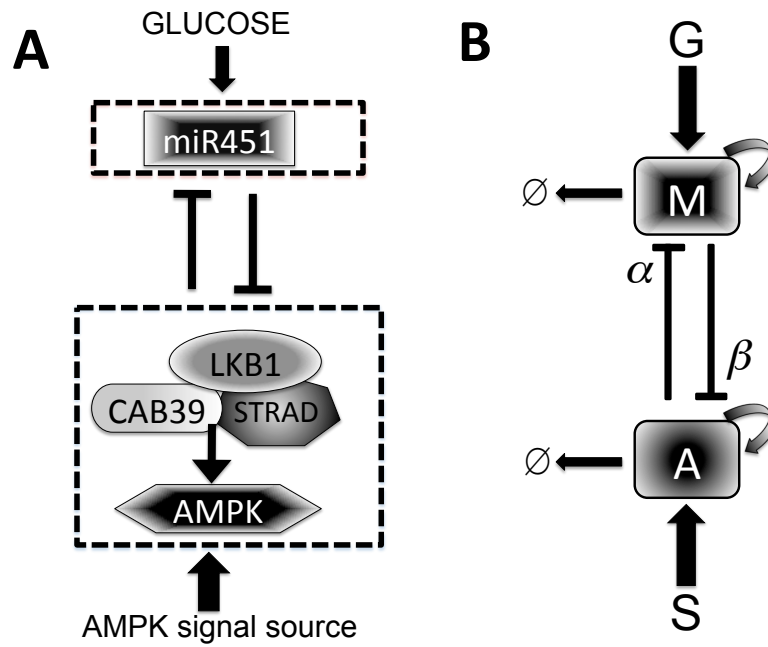
FIG. 2. (A) Conceptual model of signaling pathways and mutual antagonism of miR-451 and the AMPK complex in glioblastoma [1, 2]. (B) The dimensionless schematic diagram of the network showing mutual antagonism between miR-451 (M) and AMPK complex (A), signaling from glucose (G) and AMPK source (S) [4]. α and β are inhibition strengths and $\emptyset$ denotes decay .
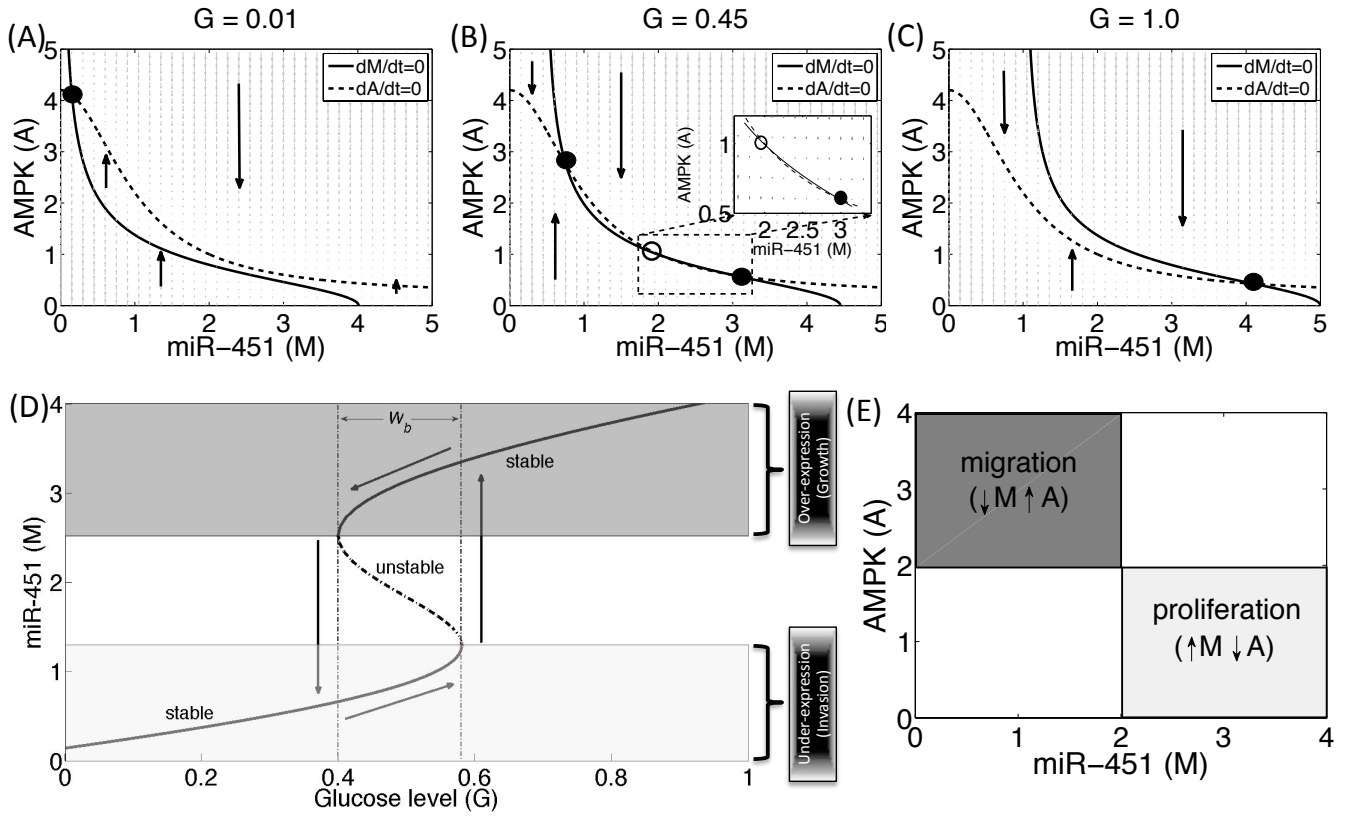
FIG. 3. (A-C) Typical dynamics of miR-451 and AMPK in response to low ($G = 0.01$ in (A)), intermediate ($G = 0.45$ in (B)) , and high ($G = 1.0$ in (C)) glucose levels. Solid line: $\frac{dM}{dt} = 0$, Dashed line: $\frac{dA}{dt} = 0$. (D) The $G - M$ hysteresis (bifurcation) curve: M is up-regulated (down-regulated) and stays in the upper (lower) stable branch in response to high (low) glucose levels (G). The system also generates a window of bi-stability ($W_b = [b_m^w, b_M^w]$) for intermediate levels of glucose ($b_m^w < G < b_M^w$) with two stable (S) steady states in the upper and lower branches and one unstable (US) steady state in a branch in the middle. Therefore, glucose levels (G) and initial conditions of M and A provide an on-off switch of miR-451 over-expression and determine the cell fate, *i.e.*, proliferation or migration [4]. (E) Characterization of proliferation and migration in miR-451-AMPK domain [1, 4]. The proliferative (Z_p) and migratory (Z_m) regions are defined as $Z_p = \{(M,A) \in \mathbb{R}^2 : M > th_M, A < th_A\}$, $Z_m = \{(M,A) \in \mathbb{R}^2 : M < th_M, A > th_A\}$, respectively. Here, th_M=2.0, th_A=2.0 [1, 4].